Seasonality in spatial variability and influence of land use/land cover and watershed characteristics on stream water nitrate concentrations in a developing watershed in the Rocky Mountain West

Kristin K. Gardner[1] and Brian L. McGlynn[1]

Received 26 March 2008; revised 5 February 2009; accepted 31 March 2009; published 11 August 2009.

[1] In recent decades, the Rocky Mountain West has been one of the fastest growing regions in the United States. Headwater streams in mountain environments may be particularly susceptible to nitrogen enrichment from residential and resort development. We utilized stream water chemistry from six synoptic sampling campaigns combined with land use/land cover (LULC) and terrain analysis in geostatistical modeling to examine the spatial and seasonal variability of LULC impacts on stream water nitrate. Stream water nitrate was spatially correlated for longer distances during the dormant season than during the growing season, suggesting the importance of biological retention. Spatial linear models indicated that anthropogenic sources best predicted stream water nitrate in the dormant season, while variables describing biological processing were the best predictors in the growing season. This work demonstrates the importance of (1) incorporating spatial relationships into water quality modeling and (2) investigating stream water chemistry across seasons to gain a more complete understanding of development impacts on stream water quality.

Citation: Gardner, K. K., and B. L. McGlynn (2009), Seasonality in spatial variability and influence of land use/land cover and watershed characteristics on stream water nitrate concentrations in a developing watershed in the Rocky Mountain West, *Water Resour. Res.*, *45*, W08411, doi:10.1029/2008WR007029.

1. Introduction

[2] Human alteration of the patterns of land use/land cover (LULC) on the earth surface is one of the most profound impacts on the functioning of natural ecosystems [*Steffen et al.*, 2004]. Impacts on water quality, commonly viewed as an integrated environmental indicator of ecosystem function, are of particular concern in high-elevation ecosystems owing to the combined effects of increased precipitation, steep slopes, limited vegetation, large areas of exposed bedrock, and shallow soils, often resulting in rapid hydrological flushing during snowmelt and rainfall [*Williams et al.*, 1993; *Forney et al.*, 2001]. Stream water nitrogen (N) concentrations and yields across the U.S. have generally increased with anthropogenic development and have been well documented [*Eckhardt and Stackelberg*, 1995; *Nolan*, 2001; *Whitehead et al.*, 2002; *Biggs et al.*, 2004; *Groffman et al.*, 2004; *Gardner and Vogel*, 2005; *Mueller and Spahr*, 2006]. However, the extent and magnitude of development impacts on stream water N concentrations vary.

[3] Spatial and seasonal variability in headwater stream N is primarily a function of watershed hydrology [*Fisher et al.*, 2004; *Meixner et al.*, 2007], physical and chemical properties of the landscape (e.g., climate, geology) [*Holloway et al.*, 1999; *Howarth et al.*, 2006], N loading (e.g., atmospheric, fertilizer, wastewater) [*Galloway et al.*, 2004], physical sorption [*Triska et al.*, 1994] and the net result of uptake, retention, and release by biota [*Stumm and Morgan*, 1996]. Identifying the spatial and seasonal variability of LULC impacts on stream water N represents a significant challenge and highlights a fundamental gap in understanding of LULC impacts on watershed N export. Addressing this need is critical to assessing the potential risk of development and effectively managing water quality at the watershed scale.

[4] Anthropogenic development can increase watershed N export by adding N from septic and wastewater effluent, fertilizer, land clearing, and animal waste [*Puckett*, 1994] and clearing vegetation and disturbing soils [*Vitousek et al.*, 1979]. The relationship between terrestrial N loading and stream N concentration is complicated because N is not conservative; there is potential for N loading to be immobilized in terrestrial and stream ecosystems. N immobilization alters the timing, magnitude, and form of N transported creating complex spatial patterns in stream water N. Mechanisms for N immobilization include: (1) microbial denitrification [*Brooks et al.*, 1996; *Burt et al.*, 1999], (2) plant or microbial assimilation [*Hadas et al.*, 1992; *Wetzel*, 2001], (3) physical sorption [*Triska et al.*, 1994], and (4) biotic and abiotic retention through iron and sulfur reduction [*Brunet and Garcia-Gil*, 1996; *Davidson et al.*, 2003].

[5] Stream and riparian ecosystems can be hot spots for N immobilization [*Lowrance et al.*, 1984; *Meyer et al.*, 1988; *Groffman et al.*, 1996; *Hill*, 1996; *Alexander et al.*, 2000; *Peterson et al.*, 2001; *Bernhardt et al.*, 2005]. The potential for N immobilization in riparian zone can be limited if: (1) hydrological flowpaths bypass the riparian zone, (2) cold temperatures limit assimilation/denitrification, or (3) there is

[1]Department of Land Resources and Environmental Sciences, Montana State University, Bozeman, Montana, USA.

0043-1397/09/2008WR007029

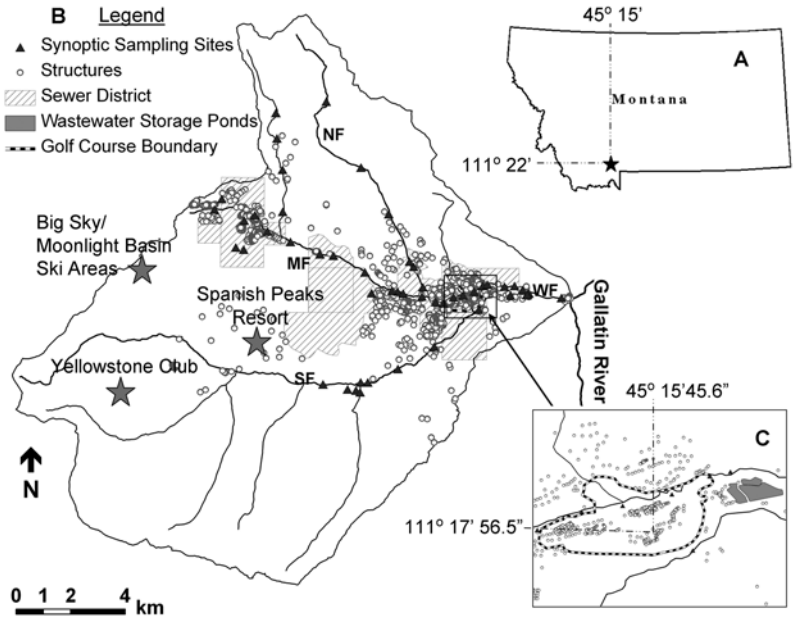

Figure 1. (a) Location of the West Fork watershed (212 km^2) in southwestern Montana. (b) Map of the West Fork watershed showing locations of 50 synoptic sampling sites, building structures, and the Big Sky Water and Sewer District boundaries. The West Fork (WF) drains into the Gallatin River (a tributary of the Upper Missouri River) and comprises three main tributaries: the Middle Fork (MF), the North Fork (NF), and the South Fork (SF). (c) An expanded view of the wastewater storage ponds and the Big Sky Resort Golf Course. Wastewater effluent is stored in the ponds and irrigated onto the golf course from mid-May through early October.

a lack of labile carbon required for microbial denitrification [*Burt et al.*, 1999; *Dent et al.*, 2007]. Research has suggested that the magnitude of instream N immobilization is controlled by stream order, concentration, and seasonality. Headwater streams are important sites for N processing and retention [*Alexander et al.*, 2000; *Peterson et al.*, 2001]; however, as uptake efficiency in small streams decreases, there is a rise in the relative role of NO_3^- removal in larger streams [*Mulholland et al.*, 2008]. Although there can be substantial processing of N in streams, there may also be concentration and seasonal thresholds, that when exceeded, the system loses its ability to remove/retain dissolved inorganic N [*Alexander et al.*, 2000; *Dodds et al.*, 2002; *Earl et al.*, 2006] similar to terrestrial environments [*Aber et al.*, 1989]. Increased watershed N loading can lead to greater N export to the stream ecosystem with instream uptake velocity decreasing as the stream approaches N saturation [*Earl et al.*, 2006], all leading to greater watershed N export. Shortest nutrient uptake lengths and highest uptake velocities generally occur in spring and summer [*Simon et al.*, 2005].

[6] Research in the Rocky Mountain West has indicated peak inorganic N concentrations occur throughout the winter and decline considerably during the growing season, suggesting the importance of N immobilization [*Williams and Melack*, 1991; *Baron and Campbell*, 1997; *Campbell et al.*, 2000; *Kaushal and Lewis*, 2003]. There is potential to increase winter N delivery to streams in mountain resort areas because human activity often peaks during the winter ski season [*Kaushal et al.*, 2006]. In the winter increased septic system effluent can leach into shallow, cold soil that has little or no capacity to transform and assimilate nutrients or retain large inputs of subsurface water; N may then directly enter shallow groundwater and be readily transported to streams [*Firestone*, 1982].

[7] Over the past decade, the Rocky Mountain West has been one of the fastest growing regions in the country (see F. Hobbs and N. Stoops, Demographic trends in the 20th century: Census 2000 special reports, 2002, available at http://www.census.gov/prod/2002pubs/censr-4.pdf). With future development, there is the potential to increase watershed N loading to sensitive mountain environments, which may already be showing signs of nitrogen enrichment [*Kaushal et al.*, 2006]. Identifying the spatial and seasonal variability of LULC impacts on stream water N represents a significant challenge; however, addressing this need is critical to accurate modeling and prediction of stream water N concentrations under changing landscape and/or climatic conditions. In this study, we investigated the spatial and seasonal variability of LULC and watershed characteristics influence on stream water N concentrations in a developing, high-elevation mountain watershed. We utilized stream water chemistry from six spatial snapshots in time combined with LULC mapping and terrain analysis in a 212 km^2 northern Rocky Mountain watershed undergoing significant LULC change to address the following questions: (1) Is there seasonality in the spatial pattern of stream water N? (2) What is the influence of LULC and watershed characteristics on stream water N and do the influences change seasonally? (3) What is the role of the spatial location of N loading?

2. Study Area

[8] The West Fork of the Gallatin River in the northern Rocky Mountains of southwestern Montana (Figure 1a)

Table 1. Synoptic Sampling Event Dates and Corresponding Hydrological Condition and Biological Activity Potential

Synoptic Date	Hydrological Conditions	Biological Activity
10 Sep 2005	base flow	high potential
12 Feb 2006	base flow	low potential
11 Jun 2006	snowmelt	medium potential
16 Oct 2006	base flow	medium to low potential
25 Mar 2007	presnowmelt	low potential
7 Aug 2007	base flow	high potential

drains Big Sky, Moonlight Basin, Yellowstone Club, and Spanish Peaks resort areas (Figure 1b). The West Fork watershed (212 km^2) is characterized by well-defined steep topography and shallow soils. Elevation in the drainage ranges from approximately 1800 to 3400 m and average annual precipitation exceeds 127 cm at higher elevations and is less than 50 cm near the watershed outlet. Sixty percent of precipitation falls during the winter and spring months (see http://www.wcc.nrcs.usda.gov/snow/snotel-data.html). Hydrographs of the West Fork River indicate peak flows during spring snowmelt typically occurring in late May/early June followed by a general recession throughout the summer, autumn, and winter months.

[9] Streams in the West Fork watershed range from first-order, high-gradient, boulder-dominated mountain streams in the upper elevations to fourth-order, alluvial streams near the watershed outlet. Stream productivity is generally low owing to cold temperatures and short growing seasons (see http://www.fs.fed.us); however, in recent years, increased algal growth has been noted in streams draining developed subwatersheds near the watershed outlet. Chlorophyll a data collected in September 2005 suggest that algal growth is elevated above natural background levels in streams draining developed subwatersheds. Median Chlorophyll a ranges from 2.5 mg/m^2 in pristine low-order streams, 20 mg/m^2 in pristine higher-order streams to 360 mg/m^2 in higher-order streams draining more developed watersheds [*Post, Buckley, Schuh, and Jernigan, Inc.*, 2005].

[10] Diverse geologic materials are present in the West Fork watershed, including metamorphosed volcanics of Archean age, sedimentary and metasedimentary formations of various ages, and colluvium and glacial deposits that dominate the surficial geology in valley bottoms. Carbonaceous minerals such as limestones and shales are present in the mineralogy of some but not all headwater catchments, and quartzite, biotite, gneiss, gabbros, and sandstones are also present [*Alt and Hyndman*, 1986; *Kellog and Williams*, 2005]. The chemical weathering potential of different minerals found throughout the study watershed is the focus of a current investigation. However, previous research has shown that inorganic N can be weathered from layered silicates such as biotite and muscovite, and sedimentary rocks such as shale [*Holloway et al.*, 1999, 2001]. Vegetation below tree line consists of coniferous forest (Lodgepole pine, Blue and Engelmann spruce, and Douglas fir), grasslands, shrublands, and willow and aspen groves in the riparian areas. The watershed has a brief growing season from mid-June through mid-September (75–90 frost free days), decreasing with elevation (U.S. Forest Service, 1994; see http://www.fs.fed.us/land/pubs/ecoregions).

[11] Big Sky Resort was established in the early 1970s and since then, the West Fork watershed has seen a rapid increase in growth with the addition of three new ski resorts and golf courses with associated residential development. Since resort development, stream water N concentrations in the West Fork of the Gallatin River have followed a similar upward trend as development [*National Science Foundation* (*NSF*), 1976] (see also Blue Water Task Force, unpublished data, 2000–2005 and Big Sky Water and Sewer District, unpublished data, 1994–1999). The Big Sky Water and Sewer District services the two village areas with public water supply and sewer (Figure 1b). Public wastewater receives secondary treatment and is stored in 3 sewer detention ponds until late spring when it is released as irrigation water onto the Big Sky Golf Course (Figure 1c). Golf course irrigation begins in midspring when the ground thaws and continues through midfall, when the ground again freezes. Areas outside of the sewer district are on individual or community septic systems and private wells (R. Edwards, personal communication, 2007).

3. Methods

3.1. Synoptic Stream Water Sampling and Chemistry Analysis

[12] The spatial distribution of watershed N export was explored through synoptic, or "snapshot-in-time," sampling in which stream water was collected in 250 mL high-density polyethylene (HDPE) bottles from 50 sites across the West Fork watershed within 2–3 h time (Figure 1b). Six repeated synoptic sampling campaigns were conducted to capture varying hydrological conditions and potential for biological activity (Table 1). Potential biological activity was assumed to be a function of stream water and air temperature. Synoptic sampling campaigns conducted in the growing season, mid-June through mid-September, were considered "high potential," while the midwinter synoptic sampling campaign was considered "low potential." Synoptic sampling sites were randomly selected to represent a range of subwatershed characteristics including: LULC, number of wastewater disposal units, geology, stream order, elevation, and discharge (Figure 1b).

[13] Stream water samples were chilled and transported to the laboratory where they were filtered within 24 h of collection with 0.45 μm Millipore Isopore Polycarbonate membranes. Filtered water samples were preserved in HDPE bottles at 0–4°C until analysis. Aqueous nitrogen species analyzed included nitrite (NO_2^-), nitrate (NO_3^-), ammonium (NH_4^+), and organic forms. Water samples collected for this study were analyzed for all major N species; however, most samples contained NO_2^- and NH_4^+ levels near or below detection limits (5–10 μg/L). We focused on NO_3^- in this study. NO_3^- was analyzed by ion-exchange chromatography (IC) using a Metrohm Peak model 820 interface equipped with a 4-mm anion-exchange column [Metrohm, Herisau, Switzerland]. Detection limits for NO_3^- were 0.011 mg/L NO_3^--N. Accuracy was within 10% for certified 0.4 ppm NO_3^--N standards (0.09 ± 0.009 mg · L^{-1} NO_3^--N), as measured every 11th sample. Coefficients of variation (CVs) for NO_3^- standard peak areas were 2% or less.

[14] A subset of the filtered stream water samples were frozen until delivery to the Woods Hole Whole Marine Microbial Biogeochemistry Lab for isotopic analysis. $\delta^{15}N$ and $\delta^{18}O$ of NO_3^- were analyzed by the Sigman-Casciotti

Table 2. Potential Explanatory Variables of Stream Water NO_3^- in the West Fork Watershed

Variable	Description
Septic	number of septics
Septic*TT*	number of septics weighed by travel time, *TT*
Septic*D*	number of septics weighted by distance to the stream, *D*
Wastewater	indicator variable (1 or 0) of wastewater loading
Area	area of subwatershed (km)
Geology	percent geology with higher N weathering potential.
Riparian buffer	ratio of riparian area to hillslope area
Forest	percent forest coverage
Order	Strahler stream order
Slope	median slope
Aspect	median aspect
Elevation	elevation at synoptic sampling site

microbial denitrifier method [*Sigman et al.*, 2001; *Casciotti et al.*, 2002]. Nitrate δ^{15}N and δ^{18}O were calibrated against USGS32, USGS34, and USGS35 [*Casciotti et al.*, 2007].

3.2. Terrain Analysis

[15] The potential impact of LULC along hydrologic flowpaths is partially controlled by landscape characteristics [*Dunne*, 1978; *Newson*, 1997]. LULC change can alter water flow and biogeochemical processes, which together mediate N movement and transformation in watersheds [*Findlay et al.*, 2001; *Biggs et al.*, 2004; *Zimmermann et al.*, 2006]. Definition of hydrological flowpaths, potential travel times along each flowpath and the concomitant spatial pattern of N loading across the West Fork watershed are necessary to explain variability in stream water N. Hydrological flowpaths can be estimated by a Digital Elevation Model (DEM) terrain analysis. The West Fork watershed has steep slopes and predominately shallow soils with high hydraulic conductivities [*Soil Conservation Service*, 1978; *Montagne et al.*, 1982]. These conditions often promote shallow runoff pathways that can result in rapid NO_3^- delivery to riparian zones and streams. Consequently, flowpaths are likely to be well represented by surface topography. For this study, the MD∞ flow accumulation algorithm [*Seibert and McGlynn*, 2007] was used to define the hydrological flowpaths in the West Fork watershed using a 10-m DEM developed by parsing a 1-m resolution Airborne Laser Swath Mapping data set.

[16] Our terrain analysis extracted relevant terrain characteristics from the 10-m DEM to use as potential predictor variables for modeling stream water (NO_3^-) concentrations. First, an approximation of water residence time for each grid cell was calculated [*McGuire et al.*, 2005]. We will refer to this approximation as water travel time (*TT*). *TT* has been shown to have a correlation of 0.91 with mean water residence time [*McGuire et al.*, 2005]. N export has been shown to be inversely related to watershed residence time by increasing the potential reaction time for immobilization [*Seitzinger et al.*, 2002]. For each grid cell, the *TT* is the hydrological flowpath distance to the stream divided by the gradient over the flowpath. Assuming a constant hydraulic conductivity throughout the watershed, *TT* can be viewed as a first approximation of Darcy's Law:

$$\overline{V} = K * I \rightarrow K = \text{a constant} \rightarrow \overline{V} \approx I \rightarrow TT \approx \frac{D}{I} \qquad (1)$$

where, $\overline{V}$ is the average velocity, K is the hydraulic conductivity, I is the gradient (slope) along the flowpath to the stream, D is the flowpath distance to the stream, and *TT* is the travel time from each grid cell to the stream following the topographically driven flow routing algorithm. Assuming this first-order approximation, *TT* is a measure of the travel time from a grid cell to the stream channel.

[17] Riparian areas were computed from the DEM by an automated method in which all area <3 m above the stream along each flowpath was delineated as a riparian zone [*McGlynn and Seibert*, 2003]. The method has been field-tested in Sleepers River, Vermont; Panola Mountain Georgia; HJ Andrews in Oregon; and at Maimai, New Zealand [*McGlynn and Seibert*, 2003; *McGlynn*, 2005]. Once riparian areas were delineated, riparian hillslope area ratios (riparian buffering potential) were computed as the ratio of local riparian area associated with each stream pixel divided by the local contributing area (lateral upslope inflows) [*McGlynn and Seibert*, 2003]. Stream reach to stream reach assessment of riparian buffering potential of lateral hillslope inputs is pertinent in LULC change-water quality analyses because it allows for assessment of potential riparian buffering down-gradient (along each flowpath) of N inputs.

[18] The subwatersheds for each of 50 synoptic stream sampling sites were delineated from the flowpath model. The 50 subwatersheds of the West Fork ranged in size from 0.04 km^2 to 207 km^2. Subwatershed characteristics were extracted to employ as potential predictor variables in spatial linear models of synoptic stream water NO_3^- concentrations (Table 2).

3.3. Statistical Analysis

3.3.1. Potential Predictor Variables

[19] Potential predictor variables were extracted for each subwatershed to describe subwatershed characteristics and LULC upstream of each synoptic sampling site (Table 2). Septic locations were mapped by masking the Big Sky Water and Sewer District boundary GIS layer over a 2006 structure layer supplied by the Gallatin County Planning District. To test the impact of septic location on watershed N export, septics were also weighted by inverse *TT* and flowpath distance to the stream (*D*). Sites influenced by wastewater input from the golf course were identified through terrain analysis and confirmed by isotopic analysis of δ^{15}N and δ^{18}O of NO_3 [*Kendall and McDonnell*, 1998].

[20] Forest cover was delineated from a cloud-free Quickbird scene acquired on 21 July 2005. Geologic maps, acquired from the Montana Bureau of Mines and Geology [*Kellog and Williams*, 2005] were used to determine the percent of geology with higher potential for N weathering in each subwatershed. The Strahler stream order classification system was used to assess stream order [*Strahler*, 1952]. Median slope, median aspect, site elevation, and area of each subwatershed were computed through terrain analysis.

3.3.2. Spatial Linear Models

[21] The unidirectional flow of water in stream networks dictates that each sampling site is influenced by upstream sites; therefore, stream water NO_3^- concentrations may not be spatially independent. The presence of spatial dependence violates the assumption of independently and identically distributed (i.i.d.) errors of most standard statistical procedures. Potentially this can encumber analyses and threatens statistical and inferential interpretation by leading to: (1) a

(a)

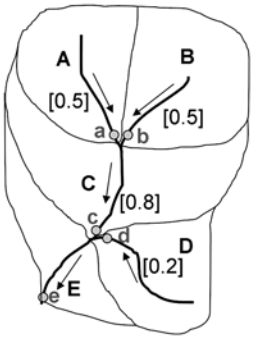

Watershed	Area
A	10
B	10
C	40
D	10
E	50

$$\text{Segment PI of A on C} = \frac{\text{Watershed area A}}{\text{Watershed area (A + B)}} = 0.5$$

(b)

TO SITE \ FROM SITE	a	b	c	d	e
a	1	0	0	0	0
b	0	1	0	0	0
c	0.5	0.5	1	0	0
d	0	0	0	1	0
e	0.4	0.4	0.8	0.2	1

Segment PI of a on e: *PI*(A)**PI*(C) = 0.4

Figure 2. A simplified example of watershed E and subwatersheds A–D to illustrate modeled spatial dependence in a stream network [after *Peterson et al.*, 2007, Figure 3]. (a) Spatial dependence of stream sites is considered only if sites are flow connected. If water flows downstream between two sites, than they are considered flow connected. Subwatersheds A and C and B and C are flow-connected sites, while A and B are not flow-connected sites. (b) The proportional influence (*PI*) matrix represents the influence of an upstream location on a downstream location. In the *PI* matrix the *PI* for a pair of sites is equal to the product of the segment *PI*s found in the path between them.

confidence interval that is too narrow, (2) underestimation of the sample variance, and (3) inaccurate parameter estimates [*Cressie*, 1993; *Legendre*, 1993]. Although spatial dependency violates standard statistical techniques, it can used as a source of information in spatial models, rather than something to be ignored or corrected [*Carroll and Pearson*, 2000].

[22] A spatial linear model is an extension of a general linear model (GLM) in which the errors are allowed to be spatially correlated. Consider the GLM: $Y = \beta X + \varepsilon$, where Y is a nx1 vector of observations, X is a nxp matrix of predictor variables, β is a px1 vector of best fit parameters, and ε is a nx1 vector of random errors. Typically, the random errors, ε, are assumed to be independent, so var $(\varepsilon) = \sigma^2 I$, where I is the nxn identity matrix. However, in spatial models, the independence assumption of ε is relaxed and the values are allowed to be spatially correlated so var $(\varepsilon) = \Sigma$, where Σ is the covariance matrix [*Cressie*, 1993]. Σ is a function of the autocovariance parameters, which are determined by fitting an autocovariance function to the modeled residuals. In order for the modeled autocovariance function to be statistically valid, it must produce a symmetric and positive-definite covariance matrix [*Cressie*, 1993].

[23] Typically, spatial models are based on Euclidian distance to quantify spatial dependence [*Cressie*, 1993]. However, Euclidian distance may not best represent distance in stream networks, and consequently, recent research has begun to use instream distance to model stream characteristics [*Dent and Grimm*, 1999; *Gardner et al.*, 2003; *Legleiter et al.*, 2003; *Ganio et al.*, 2005]. Concurrently, new geostatistical methodologies to model stream characteristics have incorporated the unidirectional flow of water by developing statistically valid covariance measures on the basis of directional hydrologic flowpath distance [*Cressie et al.*, 2006; *Ver Hoef et al.*, 2006; *Peterson et al.*, 2007]. Directional hydrologic flowpath distance may be more representative of the unidirectional flow of water and solutes in a stream network.

[24] We applied a geostatistical method, which incorporates spatial dependence of the data, using a weighted hydrologic flowpath distance developed for stream networks [*Ver Hoef et al.*, 2006]. Spatial weights are generated using metrics that represent relative influence of one site on another, such as proportion watershed area at a confluence, to create more ecologically representative distance measures [*Ver Hoef et al.*, 2006]. To implement this method, a flow network was derived from the 10 m DEM with the Functional Linkage of Waterbasins and Streams (FLoWS) toolset [*Theobald et al.*, 2005]. The flow network described whether or not a synoptic sampling site was connected to other synoptic sampling sites by streamflow. In order for two sites to be considered "flow-connected," water must flow from one site to another. If water does not flow from one site to another site (e.g., an adjacent tributary), then the sites are considered "not flow-connected" (Figure 2a).

[25] For the purpose of this study, we quantified how much influence an upstream site had on a downstream site by considering the downstream flow distance (*DFD*) between sites and the proportional influence (*PI*) of streamflow contributed from one site to another site. *DFD* is the total downstream distance between sampling sites along the flow network and the *PI* is the influence of an upstream location on a downstream location on the basis of discharge volume. For this study, watershed area was used as a surrogate for discharge volume. Watershed area has been shown to be highly correlated to annual stream discharge (R^2 values ranging from 0.92 to 0.99) in all 18 water resource regions of the United States [*Vogel et al.*, 1999]. Calculation of the *PI* of one sample site on another involves two steps [*Peterson et al.*, 2007]. First, the *PI* of each segment on the segment directly downstream is computed by dividing its watershed area by the total incoming area to the downstream segment (Figure 2b). The *PI*s of the incoming segments are proportions and will always sum to one. The second step uses the segment *PI*s to calculate the *PI* for each pair of flow-connected sites (Figure 2b). The *PI* for a pair of sites is equal to the product of the segment *PI*s found in the downstream path between them, excluding the segment *PI* that the downstream site lies on [*Peterson et al.*, 2007]. For this study, the *DFD* and *PI* matrices for each synoptic sampling campaign were computed from the flow network using the FLoWS toolset. The *DFD* and *PI* matrices must be reformatted before they can be used to create a statistically valid covariance matrix [*Peterson et al.*, 2007]. The *DFD* and *PI* matrices must be forced into symmetry by adding their respective transposes. Matrix *A* is created by taking the square root of the symmetric *PI* matrix. The symmetric *DFD*, functions as the lag distance,

and A, as a spatial weights matrix, in development of a spatial linear model.

[26] Spatial linear models for each of six synoptic campaigns were constructed by: (1) developing a spatial autocovariance model through moving average constructions on streams, (2) estimating the autocovariance parameters using restricted maximum likelihood (REML) [*Cressie*, 1993], (3) applying the covariance matrix to estimate the fixed effects by generalized least squares, and (4) making predictions using universal kriging [*Ver Hoef et al.*, 2006]. Statistically valid spatial autocovariance models for stream networks can be developed using moving average constructions on the basis of weighted hydrologic distances [*Cressie et al.*, 2006; *Ver Hoef et al.*, 2006]. The spatial autocovariance functions fitted and compared for each set of modeled parameters included the linear-with-sill, spherical, Mariah, and exponential autocovariance functions. For example, a spherical autocovariance model is:

$$C1(h|\theta_0,\theta_1,\theta_2)=\begin{cases}\theta_0+\theta_1 & If\ h=0\\ \theta_1\left[1+\frac{1}{2}\left(\frac{h}{\theta_2}\right)^3-\left(\frac{3}{2}\right)\left(\frac{h}{\theta_2}\right)\right] & If\ 0<h>\theta_2\\ 0 & If\ \theta_2\le h\end{cases} \quad (2)$$

where $C1$ is an unweighted covariance matrix not guaranteed to be statistically valid at this point [*Ver Hoef et al.*, 2006], h is hydrologic flowpath distance, and θ_0, θ_1, and θ_2 are the estimated autocovariance parameters. The autocovariance covariance parameters must be estimated in order to fit the covariance function to the empirical covariances. The estimated autocovariance parameters (and θ_0, θ_1, and θ_2) describe how the variability between data points changes with increasing separation distance. θ_0 is the "range," which is an indication of the spatial scale at which stream water N concentrations are spatially autocorrelated; beyond the range stream water NO_3^- concentrations are considered spatially independent. $\theta_1 + \theta_2$ is the "sill," which represents the variance found among uncorrelated data. θ_2 is the "nugget effect," which represents differences relating to fine-scale variability as the distance between locations approaches zero, which can result from experimental error or from variability that is occurring at a scale finer than the study scale. Finally, the partial sill, which is the difference between the sill and the nugget is the autocorrelated variation. The autocovariance parameters, θ_0, θ_1, and θ_2, were estimated by REML.

[27] Finally, the covariance matrix, Σ is computed by applying the Hadamard (element-wise) product of the unweighted covariance matrix, $C1$, and the spatial weights matrix, A [*Ver Hoef et al.*, 2006; *Cressie et al.*, 2006; *Peterson et al.*, 2007]:

$$\sum = C1 \odot A \quad (3)$$

Σ was used in the general linear model to estimate the fixed effects by generalized least squares. Model residuals were assessed to identify outliers. Extreme outliers at the 0.01 significance level were identified by studentized residuals and removed. Leave-one-out cross-validation predictions were generated to calculate the Root Mean Square Prediction Error (RMPSE) for each model [*Hastie et al.*, 2001].

[28] The "best" model for each synoptic event was selected by forward and backward stepwise selection by minimizing the RMSPE [*Hastie et al.*, 2001]. RMSPE was used in model selection because information criteria are invalid when REML is used to estimate the autocovariance parameters [*Molenberghs and Verbeke*, 2000]. If alternative models had the same RMSPE then model selection was based on maximizing the r^2 value for the observations and the cross-validation predictions.

3.3.3. Semivariogram Plots

[29] For visual interpretation, we computed semivariogram plots of the raw data and the fitted model residuals of stream water NO_3^- concentrations. Semivariograms were computed to compare the degree of similarity among samples as a function of the instream distance between them:

$$\hat{\gamma}(h)=\frac{1}{2N(h)}\sum_{i=1}^{N(h)}(z(x_i)-z(x_i+h))^2 \quad (4)$$

where $\hat{\gamma}$ (h) is the estimated semivariance at a separation distance h, $N(h)$ is the number of paired data with a range of distances (or lag) of h, $z(x_i)$ and $z(x_i + h)$ are the data at two locations, and h is the distance between pairs [*Cressie*, 1993]. If spatial correlation does exist, the semivariance increases as the distance between the sites increases. Semivariograms for flow-connected models should be interpreted with caution because there is no weighting for flow volume [*Ver Hoef et al.*, 2006].

4. Results

[30] Spatial variability of stream water NO_3^- concentrations within and across synoptic sampling campaigns is illustrated in Figures 3, 4, and 5. Seasonal synoptic concentrations were within the range of weekly NO_3^- time series of two streams, one draining a pristine watershed and the other a more developed watershed (Figure 4). Stream water NO_3^- concentrations were highest in the winter months with median concentrations in February and March of 0.17 and 0.14 mg/L-NO_3^--N, respectively. Greatest variability of stream water NO_3^- occurred in late fall, winter, and early spring, when the variance of stream water NO_3^- in October, February and March was 0.01, 0.15 and 0.08 mg/L NO_3^--N, respectively (Figures 4 and 5). NO_3^--N concentrations remained elevated at sites draining Lone Mountain (major mountain of Big Sky Resort) compared to other streams across a range of hydrologic conditions and biological potential (Figure 5). Sites downgradient from wastewater loading were significantly elevated compared to other sites during the winter/late fall (Figure 5). Isotopic analysis of $\delta^{15}N$ and $\delta^{18}O$ of NO_3^- indicate elevated $\delta^{15}N$ values, similar to the wastewater signature [*Kendall and McDonnell*, 1998], at sites located downgradient from the Big Sky golf course as compared to other sites. Semivariograms of raw stream water NO_3^- concentrations at flow-connected sites versus not flow-connected sites illustrate seasonality in the autocorrelated

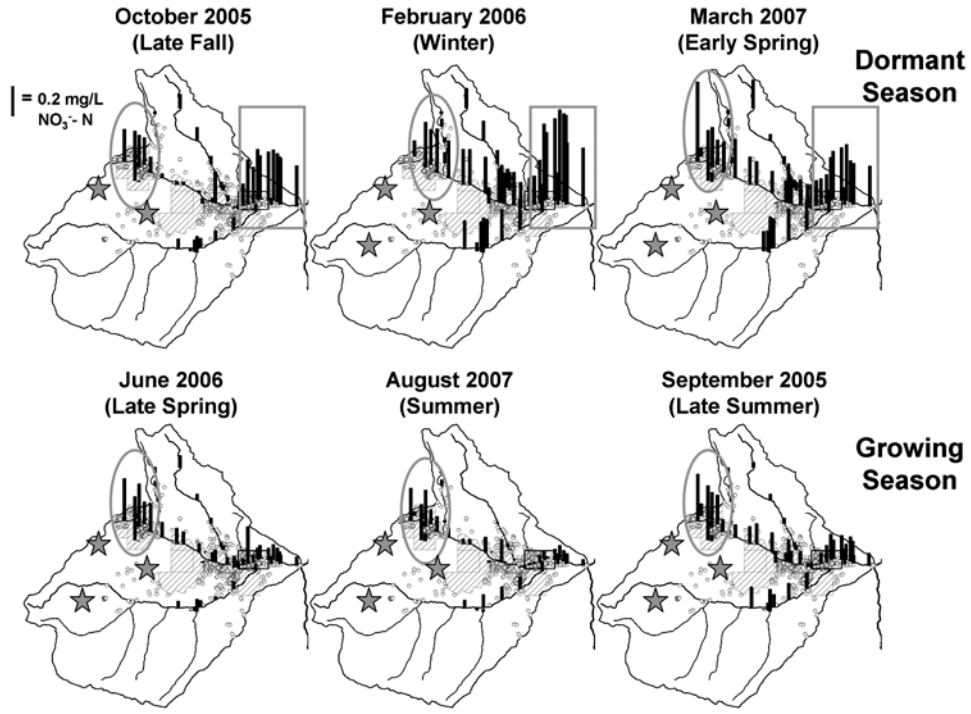

Figure 3. Stream water NO_3^- concentrations for six synoptic sampling campaigns capturing a range of seasonal, hydrological, and biological conditions (see Table 1). Elevated NO_3^- concentrations persist in streams draining Lone Mountain across seasons (gray ovals), while elevated concentrations downgradient from the Big Sky Golf Course are elevated only in the winter months during periods of low potential biologic activity (gray rectangles).

variation at flow-connected sites (Figure 6). The sill variance of flow-connected sites was greater in the late fall, winter, and early spring semivariograms as compared to late spring, summer, and late summer. Because apparent spatial structure existed in the raw data variograms, a spatial model was applied to incorporate the spatial relationships into the modeling process.

[31] Spatial linear models indicate seasonal differences in the influential roles of LULC and terrain characteristics on stream water NO_3^- (Table 3). During the late spring (June), summer (August), and late summer (September), predictor variables representative of biological processing (riparian buffer potential and percent forest) were significant predictors of stream water NO_3^- concentrations. In the late fall (October), winter (February), and early spring (March), N loading variables (i.e., septic, wastewater and geology) had the highest explanatory power of the stream water NO_3^- signal. The best model fits were in February ($r^2 = 0.90$) and

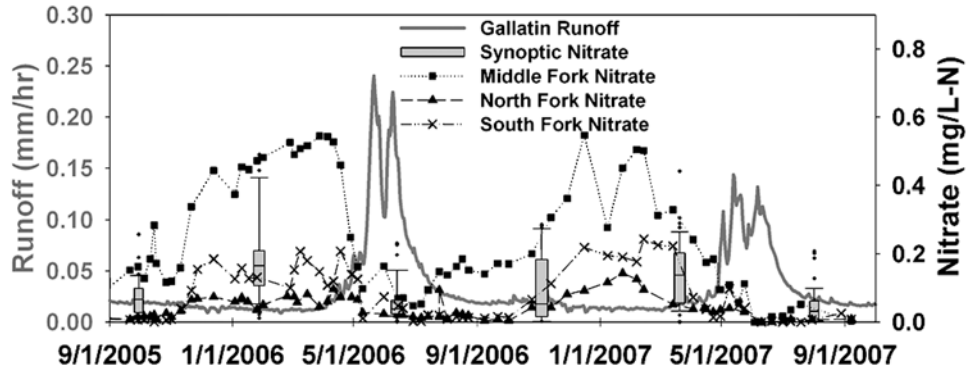

Figure 4. Synoptic NO_3^- concentrations for the six synoptic sampling campaigns conducted between September 2005 and August 2007. Each boxplot consists of 46–50 data points. Stream water NO_3^- concentrations and variability are highest during late fall, winter, and early spring during periods of low streamflow and limited biologic activity. The weekly time series for two sites with varying levels of N loading are included for context and are represented by squares (Middle Fork, high N loading), crosses (South Fork, medium N loading), and triangles (North Fork, low N loading).

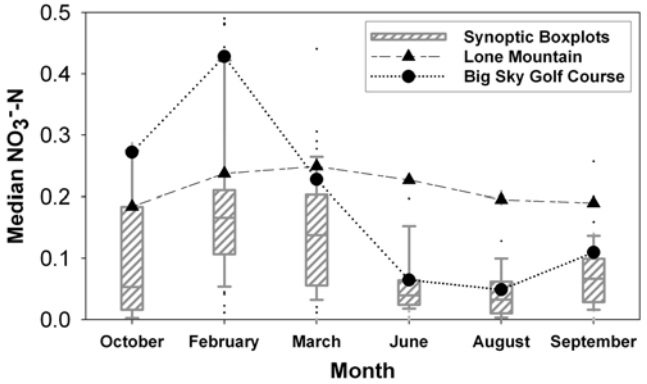

Figure 5. Median stream water NO_3^- concentrations of sites located downgradient from the Big Sky Golf Course (black circles) and Lone Mountain (black triangles) for each synoptic event (gray boxplots). Stream water NO_3^- at sites draining Lone Mountain remain relatively elevated throughout the year, while stream water NO_3^- concentrations at sites downgradient from the Big Sky Golf Course exhibit a more amplified seasonal pattern.

October (r^2 = 0 0.75). The least amount of variability was explained in the June and March when model fits (r^2) were 0.06 and 0.37, respectively. In midsummer (August), only one of the N loading variables was significant in predicting stream water NO_3^-, while in the midwinter (February) all of the N loading variables were significant (Table 3).

[32] The estimated covariance parameters of the spatial modeling residual semivariograms signify seasonality in the range parameter (see Table 4 and Figure 7). The range is longest in October and February at 5.03 and 5.51 km respectively, and lowest in the August and June, when the range

Table 3. Spatial Linear Models Fitted to Stream Water NO_3^- for Each Synoptic Sampling Campaign[a]

Explanatory Variables	Coefficient	*p* Value	r^2	RMPSE
	Oct 2006			
Intercept	0.033	0.023	0.75	0.047
Septic*TT*	2.379	0.002		
Wastewater	0.092	<0.001		
	Feb 2006			
Intercept	0.085	<0.001	0.90	0.037
Septic	0.0005	<0.001		
Wastewater	0.221	<0.001		
Geology	40.0	0.008		
	Mar 2007			
Intercept	0.083	<0.001	0.37	0.059
Septic*TT*	1.942	<0.001		
	Jun 2006			
Intercept	0.209	<0.001	0.06	0.045
Septic *TT*	1.437	0.002		
Riparian buffer potential	−1.441	0.004		
Stream order	−0.033	0.006		
Forest	−0.135	0.027		
	Aug 2007			
Geology	53.5	<0.0001	0.53	0.0203
Forest	−0.117	0.003		
	Sep 2005			
Intercept	0.139	<0.001	0.45	0.028
Geology	45.42	<0.001		
Wastewater	0.058	<0.001		
Forest	−0.018	<0.001		
Riparian buffer potential	−0.626	0.077		

[a]See Table 2 for variable descriptions.

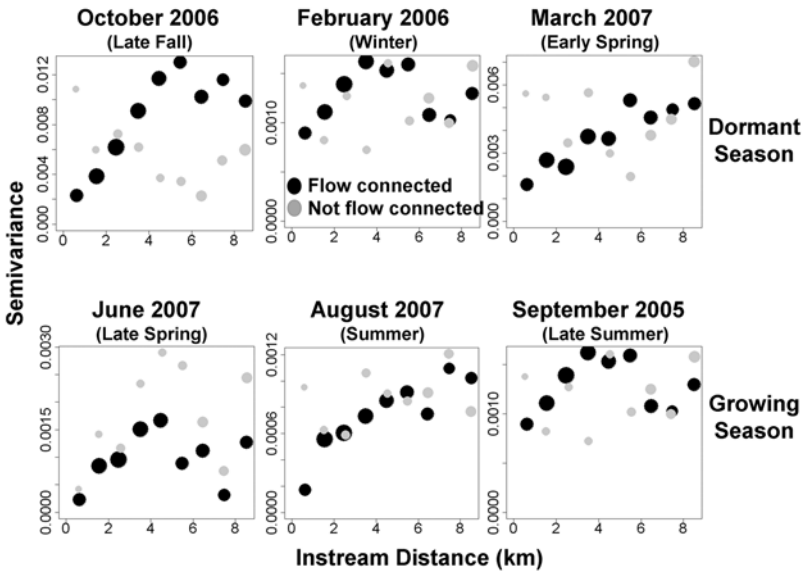

Figure 6. Semivariograms of unmodeled synoptic stream water NO_3^-. Seasonality exists in the degree autocovariance variance between flow-connected sites (black circles) and is not apparent in not flow-connected sites (gray circles). Dormant season semivariograms (February, winter; October, late fall; and March, early spring) illustrate a greater autocorrelated variance than growing season (June, late spring; August, summer; and September, late summer). This difference in autocorrelated variability suggests the importance of a biologic component in stream water NO_3^- patterns during periods of high potential biologic activity. Symbol size is proportional to the number of pairs at each lag distance.

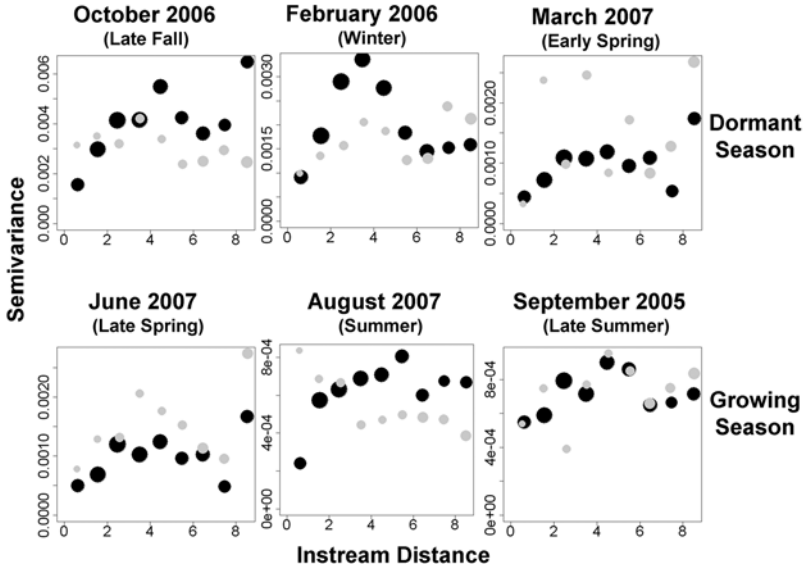

Figure 7. Semivariograms of the spatial model residuals of synoptic stream water NO_3^-. Seasonality exists in the range of spatial dependence between flow-connected sites (black circles) and is not apparent in not flow-connected sites (gray circles). The range of spatial dependency is longer in the dormant season (February, winter; October, late fall; and March, early spring) as compared to the growing season (June, late spring; August, summer; and September, late summer). The shorter range in the growing season suggests the importance of a biologic component in stream water NO_3^- patterns during periods of high potential biologic activity. Symbol size is proportional to the number of pairs at each lag distance.

was 2.18 and 1.88, respectively. The nugget was generally low for all models, ranging from 0.00007 to 0.002.

5. Discussion

[33] The extensive spatial stream water chemistry data collected over six time periods covering a range of hydrological conditions and potential biological activity in the West Fork watershed is a valuable and unique data set for exploring spatiotemporal trends in stream water N export and assessing water quality impacts of mountain resort development. Furthermore, this study is the first study to use extensive spatial data sets across time employing geostatistical models on the basis of flow-connected hydrologic distance measures to examine trends in spatial patterns and seasonal controls of stream water chemistry.

[34] Spatial and temporal data indicated that peak stream water NO_3^- concentrations in both pristine and developed watersheds occur throughout the winter and decline during the growing season (Figures 3, 4, and 5), which is consistent with other research in mountainous areas throughout the Rocky Mountain West [*Williams and Melack*, 1991; *Baron and Campbell*, 1997; *Campbell et al.*, 2000; *Kaushal and Lewis*, 2003, *Kaushal et al.*, 2006]. The magnitude of the winter peak was greater in developed watersheds and highest at sites downgradient from wastewater loading on the Big Sky Golf Course (Figures 3, 4, and 5).

5.1. Is There Seasonality in the Spatial Pattern of Stream Water N?

[35] Spatial heterogeneity of stream water NO_3^- concentrations existed within and across synoptic events (Figures 3, 4, and 5). Stream water NO_3^- concentrations remained elevated at sites draining Lone Mountain (Big Sky Resort/Moonlight Basin resort areas) throughout a range of hydrological conditions and potential biological potential activity (all 6 synoptic campaigns), while sites downgradient from wastewater loading at the Big Sky Golf Course were only elevated during the winter and late fall synoptics (Figures 3 and 5). Much of Lone Mountain is an alpine environment above treeline with steep slopes, consisting mainly of talus and scree. There is limited vegetation below treeline as a result of ski runs and resort development. Riparian areas are small in these subwatersheds. Conversely, the Big Sky Golf Course is situated in an alluvial valley with abundant vegetation, deeper more developed soils, and wider riparian areas providing an environment more likely to immobilize N loading during the growing season. Elevated inorganic N concentrations draining talus and scree fields have been noted in other research [*Williams and Tonnessen*, 2000; *Clow and Sueker*, 2000; *Hood et al.*, 2003; *Seastedt et al.*, 2004]. At these high elevations, there is increased precipitation and potential for increased deposition of inorganic N in areas with shallow soils, steep talus/scree slopes, and little riparian area with limited potential for N processing. These spatial and

Table 4. Spatial Covariance Parameters for the Spatial Linear Models Fitted to Stream Water NO_3^- for Each Synoptic Sampling Campaign[a]

Synoptic Month	Autocovariance Model	Nugget	Partial Sill	Range (km)
Oct 2006	spherical	0.002	0.003	5.03
Feb 2006	exponential	0.00043	0.00098	5.505
Mar 2007	linear with sill	0.0008	0.002	3.17
Jun 2006	mariah	0.00016	0.00228	1.88
Aug 2007	linear with sill	0.00007	0.0005	2.18
Sep 2005	linear with sill	0.0004	0.0002	2.70

[a]See Table 2 for variable descriptions.

seasonal patterns suggest that N may be immobilized along upland and riparian flow paths and in the stream network during the late spring, summer, and late summer in the valley bottom; while at higher elevations on Lone Mountain, there may be limited N processing and thus, stream water NO_3^- concentrations remain elevated throughout the year (Figures 3 and 5).

[36] The distance, or range, over which stream water NO_3^- concentrations were spatially correlated differed between seasons (see Table 4 and Figure 7). The range of the semivariograms in the dormant season varied from 3.17 in March to 5.51 km in February, while during the growing season the range of the semivariograms varied from 1.88 in June to 2.70 km in September. These differences in spatial dependence, suggest that stream water NO_3^- concentrations are influenced by ecological and hydrological processes acting at different spatial and temporal scales.

[37] *Peterson et al.* [2006] found ranges to vary between 20 and 73 km in stream water NO_3^- data collected statewide in Maryland streams during the spring and summers of 1995–1997. Modeled ranges were 20.78, 45.13, and 73.30 depending on the type of distance measure used (i.e., Euclidian, symmetric hydrologic flowpath distance, and weighted asymmetric hydrologic flowpath distance, respectively). In another study using the same Maryland data set, *Yuan* [2004] used Euclidian distance measures in geostatistical models and found the range of stream water NO_3^- to be 49 km. The difference in range values found between *Peterson et al.* [2006] and *Yuan* [2004] may be a result of the differences in the methods used to fit the autocovariance functions: *Yuan* [2004] used weighed least squares, while *Peterson et al.* [2006] used maximum likelihood *Peterson et al.* [2006]. In an N-limited desert stream in Arizona, range values for stream water NO_3^- decreased with postflood successional time from >3000 m during the first succession to 359 m during the succession survey [*Dent and Grimm*, 1999]. It is difficult to compare the results of this study to those of other studies because there are regional differences in the ecological processes that affect water chemistry [*Johnes and Butterfield*, 2002; *Clark et al.*, 2000].

5.2. What Is the Influence of LULC and Watershed Characteristics on Stream Water N and Do the Influences Change Seasonally?

[38] Spatial linear models indicated seasonal shifts in the relationships between LULC and terrain variables on stream water NO_3^- concentrations (Table 3). During the dormant season, predictor variables describing the major sources of N loading (septic, wastewater, and geology) had positive relationships and were significant in predicting stream water NO_3^- concentrations. The strongest relationships occurred in the midwinter synoptic (February) when 90% of the variability in stream water NO_3^- was explained by septic, wastewater and geology, and p values for all predictor variables were significant at the 10% level (Table 3). Although wastewater was not significant in the early spring (March) synoptic model (Table 3), there was elevated stream water NO_3^- at most sites downgradient of the Big Sky Golf Course (Figure 3). The March synoptic was complicated by a period of above freezing temperatures, melting snowpack at lower elevations, and slightly elevated discharge. More snowmelt was likely occurring in watersheds drained by higher-order valley bottom streams, than in the watersheds drained by low-order high-elevation headwater streams (personal observation).

[39] During the growing seasons, the fitted modeling results suggest the importance of a biological component in predicting stream water NO_3^- (Table 3). The significance of riparian and upland vegetation in the growing season spatial models supports other research that has shown vegetation to be effective at processing watershed nutrients. Percent forest, which may be representative of upland N processing, had a significant negative relationship with stream water NO_3^- during the growing season. Riparian buffering potential was a significant predictor variable of stream water NO_3^-, with an inverse relationship in the late spring (June) and late summer (September) (Table 3). Riparian buffering potential was not a significant predictor of August, October, February, and March stream water NO_3^- concentrations; which may result from a lack of hydrologic connection between the riparian buffer and the water table [*Jencso et al.*, 2009] and/or limited biological retention (i.e., microbial and plant assimilation and microbial denitrification) occurring in riparian areas in the winter.

[40] Investigations of microbial dynamics in alpine tundra and dry meadows revealed a seasonal pattern wherein plant uptake dominates the summer growing season and maximal microbial assimilation takes place in autumn and winter under snowpack [*Brooks et al.*, 1998; *Lipson et al.*, 1999; *Sickman et al.*, 2003]. However, microbial activity is isolated in shallow soil from groundwater and deeper soil [*Brooks et al.*, 1996, 1998; *Brooks and Williams*, 1999]. These studies found that microbial biomass gradually increased through the autumn and winter, peaking at the initiation of snowmelt and declining as snowmelt progressed. Perhaps, microbial assimilation was occurring during the winter, but a lack of hydrologic connectivity between the shallow soils and the stream network may have prevented the riparian buffer from immobilizing detectable amounts of N. This may explain why riparian buffering potential was not found to be a significant predictor in spatial linear models in October, February and March stream water NO_3^-. However, in September there was a small rain event just prior and during the September synoptic sampling campaign, which may have created a riparian/upland connection and thus the potential for riparian buffering of N along hydrological flowpaths.

[41] Spatial models of June and March synoptic NO_3^- concentrations had the least amount of predictive ability. R^2 was 0.06 and 0.37, respectively, while RMSPE was 0.045 and 0.059, respectively. Both of these synoptic events occurred during significant snowmelt events. In March, snowmelt was only occurring at lower elevations, and in June, snowmelt was only occurring at higher elevations, while the lower elevations were drying out. During these hydrologic transitional periods, it may be difficult to model the watershed as a whole since elevational differences exist in hydrological and ecological processes as a result of temperature, radiation, and snow cover gradients [*Seastedt et al.*, 2004].

[42] In the West Fork watershed, development impacts were most apparent in the winter months when stream water NO_3^- concentrations downstream of N loading sources were two to three times greater than stream water NO_3^- concentrations in pristine areas (Figures 3, 4, and 5). The spatial linear models confirmed the importance of N loading on

stream water NO_3^- concentrations in the dormant season. *Aber et al.* [1989], proposed a hypothetical timeline for a watershed response to chronic, spatially distributed N loading from atmospheric deposition. Although N loading in the West Fork watershed is localized, we propose that it exhibits the same characteristics as spatially distributed N loading. According to *Aber et al.* [1989], a sequence of four recognizable stages emerges in response to long-term loading and leads to seasonal patterns of stream water NO_3^- concentrations. Stage characteristics range from stage 0, in which there is a slight seasonal pattern in stream water NO_3^- to stage 3, in which chronic yearlong elevated NO_3^- concentrations persist with no recognizable seasonal pattern. Stream water NO_3^- concentrations in the North Fork, draining a relatively pristine subwatershed, exhibit slight winter peaks and low concentrations at base flow (stage 0). Slightly amplified stream water NO_3^- winter peaks in the South Fork are characteristic of stage 1, while amplified winter and summer stream water NO_3^- concentrations downstream of wastewater loading in the Middle Fork suggest stage 2 conditions (Figure 4). We propose a modified N saturation conceptual model whereby localized N saturation along upland flowpaths leads to heterogeneity in N saturation state. In addition, this flowpath saturation and watershed N saturation state heterogeneity results in N dilution during snowmelt and highest concentrations during winter base flow.

[43] Results from this study indicate the importance of investigating across seasons to elucidate the seasonal impacts of development on stream water chemistry. Water quality studies, which focus on water quality during the "critical period" or summer base flow, may miss the early characteristics of N enrichment. Without seasonal monitoring of stream water N, watershed managers would not be aware of amplified NO_3^- peaks in the winter. Streams with low NO_3^- concentrations in the growing season may still be exhibiting signs of N enrichment with an amplified winter peak. Knowledge of an amplified seasonal N pattern, would inform watershed managers of the early stages of N enrichment, and the future potential of water quality degradation with continued or increased N loading. Moreover, a complete understanding of the nutrient status of headwater streams is critical to understand larger-scale nutrient issues. For example, the West Fork of the Gallatin flows into the Mississippi River and eventually the Gulf of Mexico, which is already experiencing water quality problems owing to nutrient enrichment.

5.3. What Is the Role of Spatial Location of N Loading?

[44] Fitted spatial linear models indicate that spatial location of septics along hydrological flowpaths (i.e., weighted by inverse *TT*) were significant in predicting stream water NO_3^- concentrations during seasonal transitions (Table 3). One would expect travel time to have an inverse relationship with stream water NO_3^- concentrations because the more time it takes N to travel to the stream, the more reaction time available for N immobilization to occur. Septic locations weighted by *TT* was a better predictor of stream water NO_3^- than unweighted septic locations in March, June, and October; while unweighted septic was a better predictor during midwinter (February) (Table 3). During August and September N loading from septics (weighted or not weighted) was not a significant explanatory variable of stream water NO_3^- concentrations. These results suggest biological processing of terrestrial N loading may be occurring during the growing season. In midwinter, when there is low potential for biological activity, terrestrial N loading leaches through cold soils to groundwater and is readily transported to the stream, while during the growing period with highest potential for biological activity (August and September), N immobilization (assimilation and denitrification) along hydrological flowpaths mediates N transport to the stream. In August and September, septic N loading may be immobilized along hydrological pathways before it reaches the stream network or a lack of hydrological connection may prohibit N transport to the stream network [*Jencso et al.*, 2009].

[45] Another way to examine the role of spatial location of N loading is to focus on the stream network. In other words, does N loading along the stream network have cascading impacts on stream water NO_3^- concentrations downstream? Similar to the terrestrial impacts of N loading on stream water NO_3^-, the impact of spatial location of N loading along the stream network depends on the time of year. During the growing season, semivariograms indicate that N loading along the stream network had less downstream impact on stream water stream water NO_3^- concentrations than during the dormant season (see Figure 7 and Table 4). These results suggest N immobilization along upland and riparian flow paths and/or in the stream network may lead to a breakdown in spatial pattern and a lack of spatial correlation, therefore partially mitigating potential downstream impacts of N loading during the growing season.

[46] Ongoing research in the West Fork watershed will further explore the spatial and seasonal patterns of LULC and watershed characteristics influences on stream water NO_3^- by: (1) quantifying instream biological immobilization through space, seasons, and ambient N concentration via instream N additions across the West Fork watershed, (2) determining N weathering potential of geologic materials in the West Fork watershed, and (3) conducting spatially semi-distributed analyses and modeling.

6. Conclusion

[47] Synoptic sampling approaches in the West Fork watershed of southwestern Montana provided evidence that spatial and seasonal variability exists in the influences of LULC and watershed characteristics on stream water quality. This research suggests that at lower elevations during periods of high biological potential, N immobilization may lead to a breakdown of spatial stream water N patterns, therefore masking or potentially inhibiting LULC impacts on stream water NO_3^- concentrations. However, in high-elevation alpine environments, N concentrations remained elevated yearlong.

[48] Spatial linear models indicate that there are seasonal differences in the range of spatial autocorrelation of synoptic stream water NO_3^- concentrations: stream water NO_3^- concentrations are spatially correlated at a larger scale during the dormant season as compared to the growing season. Spatial linear models of stream water NO_3^- revealed seasonal shifts in the influence of LULC and watershed characteristics on stream water NO_3^-. In the dormant season, N loading variables explained the most variability in stream water NO_3^- concentrations, while during the growing season, riparian buffering potential and percent forest most strongly influ-

enced stream water NO_3^-. This study provides valuable insight into the spatial and seasonal influences of LULC impacts on stream water NO_3^- concentrations and variability in mountain streams. As populations in the Rocky Mountain West continue to rise, incorporating spatial dependence and seasonality into water quality models will be critical to accurately predict the impact of future development scenarios and the ramifications of changing climatic conditions.

[49] **Acknowledgments.** Financial support was provided by the Environmental Protections Agency (EPA) STAR grant R832449, EPA 319 funds administered by the Montana Department of Environmental Quality; the U.S. National Science Foundation (NSF) BCS 0518429; and the USGS 104(b) grant program administered by the Montana Water Center. We appreciate the critical reviews of Erin Peterson, Mark Williams, and an anonymous reviewer. K. K. G. acknowledges support from the EPA STAR Fellowship and NSF GK-12 Fellowship programs. We thank the Big Sky community for allowing access to sampling sites, in particular the Big Sky Water and Sewer District and Big Sky and Moonlight ski resort areas.

References

Aber, J. D., K. J. Nadelhoffer, P. Steudler, and J. M. Melillo (1989), Nitrogen saturation in northern forest ecosystems: Excess nitrogen from fossil fuel combustion may stress the biosphere, *BioScience*, *39*(6), 378–385, doi:10.2307/1311067.

Alexander, R. B., R. A. Smith, and G. E. Schwarz (2000), Effect of stream channel size on the delivery of nitrogen to the Gulf of Mexico, *Nature*, *403*, 758–761, doi:10.1038/35001562.

Alt, D., and D. W. Hyndman (1986), *Roadside Geology of Montana*, Mountain Press, Missoula, Mont.

Baron, J. S., and D. H. Campbell (1997), Nitrogen fluxes in a high elevation Colorado Rocky Mountain basin, *Hydrol. Processes*, *11*, 783–799, doi:10.1002/(SICI)1099-1085(199706)11:7<783::AID-HYP519>3.0.CO;2-U.

Bernhardt, E. S., et al. (2005), Can't see the forest for the stream? Instream processing and terrestrial nitrogen exports, *BioScience*, *55*(3), 219–230, doi:10.1641/0006-3568(2005)055[0219:ACSTFF]2.0.CO;2.

Biggs, T. W., T. Dunne, and L. A. Martinelli (2004), Natural controls and human impacts on stream nutrient concentrations in a deforested region of the Brazilian Amazon basin, *Biogeochemistry*, *68*, 227–257, doi:10.1023/B:BIOG.0000025744.78309.2e.

Brooks, P. D., and M. W. Williams (1999), Snowpack controls on nitrogen cycling and export in seasonally snow-covered catchments, *Hydrol. Processes*, *13*, 2177–2190, doi:10.1002/(SICI)1099-1085(199910)13:14/15<2177::AID-HYP850>3.0.CO;2-V.

Brooks, P. D., M. W. Williams, and S. K. Schmidt (1996), Microbial activity under alpine snowpacks, Niwot Ridge, Colorado, *Biogeochemistry*, *32*, 93–113, doi:10.1007/BF00000354.

Brooks, P. D., M. W. Williams, and S. K. Schmidt (1998), Inorganic nitrogen and microbial biomass dynamics before and during spring snowmelt, *Biogeochemistry*, *43*, 1–15, doi:10.1023/A:1005947511910.

Brunet, R. C., and L. J. Garcia-Gil (1996), Sulfide-induced dissimilatory nitrate reduction to ammonia in anaerobic freshwater sediments, *FEMS Microbiol. Ecol.*, *21*, 131–138, doi:10.1111/j.1574-6941.1996.tb00340.x.

Burt, T. P., L. S. Matchett, K. W. T. Goulding, C. P. Webster, and N. E. Haycock (1999), Denitrification in riparian buffer zones: The role of floodplain hydrology, *Hydrol. Processes*, *13*, 1451–1463, doi:10.1002/(SICI)1099-1085(199907)13:10<1451::AID-HYP822>3.0.CO;2-W.

Campbell, D. H., J. S. Baron, K. A. Tonnessen, P. D. Brooks, and P. F. Schuster (2000), Controls on nitrogen flux in alpine/subalpine watersheds of Colorado, *Water Resour. Res.*, *36*, 37–47.

Carroll, S. S., and D. L. Pearson (2000), Detecting and modeling spatial and temporal dependence in conservation biology, *Conserv. Biol.*, *14*(6), 1893–1897, doi:10.1046/j.1523-1739.2000.99432.x.

Casciotti, K. L., D. M. Sigman, M. G. Hastings, J. K. Bohlke, and A. Hilkert (2002), Measurement of the oxygen isotopic composition of nitrate in seawater and freshwater using the denitrifier method, *Anal. Chem.*, *74*(19), 4905–4912, doi:10.1021/ac020113w.

Casciotti, K. L., J. K. Bohlke, M. R. McIlvin, S. J. Mroczkowski, and J. E. Hannon (2007), Oxygen isotopes in nitrite: Analysis, calibration, and equilibration, *Anal. Chem.*, *79*(6), 2427–2436, doi:10.1021/ac061598h.

Clark, G. M., D. K. Mueller, and M. A. Mast (2000), Nutrient concentrations and yields in undeveloped stream basins of the Unites States, *J. Am. Water Resour. Assoc.*, *36*(4), 849–860, doi:10.1111/j.1752-1688.2000.tb04311.x.

Clow, D. W., and J. K. Sueker (2000), Relations between basin characteristics and stream water chemistry in alpine/subalpine basins in Rocky Mountain National Park, Colorado, *Water Resour. Res.*, *36*, 49–61, doi:10.1029/1999WR900294.

Cressie, N. (1993), *Statistics for Spatial Data*, John Wiley, Hoboken, N. J.

Cressie, N., J. Frey, B. Harch, and M. Smith (2006), Spatial prediction on a river network, *J. Agric. Biol. Environ. Stat.*, *11*(2), 127–150, doi:10.1198/108571106X110649.

Davidson, E. A., J. Chorover, and D. B. Dail (2003), A mechanism of abiotic immobilization of nitrate in forest ecosystems: The ferrous wheel hypothesis, *Global Change Biol.*, *9*, 228–236, doi:10.1046/j.1365-2486.2003.00592.x.

Dent, C. L., and N. B. Grimm (1999), Spatial heterogeneity of stream water nutrient concentrations over successional time, *Ecology*, *80*, 2283–2298.

Dent, C. L., N. B. Grimm, E. Marti, J. W. Edmonds, J. C. Henry, and J. R. Welter (2007), Variability in surface-subsurface hydrologic interactions and implications for nutrient retention in an arid-land stream, *J. Geophys. Res.*, *112*, G04004, doi:10.1029/2007JG000467.

Dodds, W. K., et al. (2002), N uptake as a function of concentration in streams, *J. N. Am. Benthol. Soc.*, *21*, 206–220, doi:10.2307/1468410.

Dunne, T. (1978), Field studies of hillslope processes, in *Hillslope Hydrology*, edited by M. J. Kirkby, pp. 227–289, John Wiley, Hoboken, N. J.

Earl, S. R., H. M. Valett, and J. R. Webster (2006), Nitrogen saturation in streams, *Ecology*, *87*, 3140–3151, doi:10.1890/0012-9658(2006)87[3140:NSISE]2.0.CO;2.

Eckhardt, D. A., and P. E. Stackelberg (1995), Relation of ground-water quality to land use on Long Island, New York, *Ground Water*, *33*(6), 1019–1033, doi:10.1111/j.1745-6584.1995.tb00047.x.

Findlay, S., J. M. Quinn, C. W. Hickey, G. Burrell, and M. Downes (2001), Effects of land use and riparian flowpath on delivery of dissolved organic carbon to streams, *Limnol. Oceanogr.*, *46*(2), 345–355.

Firestone, M. K. (1982), Biological denitrification, in *Nitrogen in Agricultural Soils*, *Agron. Monogr. Ser.*, vol. 22, edited by F. J. Stevenson, pp. 289–326, Am. Soc. of Agron., Madison, Wisc.

Fisher, S., R. Sponseller, and J. Heffernan (2004), Horizons in stream biogeochemistry: Flowpaths to progress, *Ecology*, *85*, 2369–2379, doi:10.1890/03-0244.

Forney, W., L. Richards, K. D. Adams, T. B. Minor, T. G. Rowe, J. LaRue Smith, and C. G. Raumann (2001), Land use change and effects on water quality and ecosystem health in the Lake Tahoe Basin, Nevada and California, *U. S. Geol. Surv. Open File Rep.*, *01-418*.

Galloway, J. N., et al. (2004), Nitrogen cycles: Past, present, and future, *Biogeochemistry*, *70*, 153–226, doi:10.1007/s10533-004-0370-0.

Ganio, L. M., C. E. Torgersen, and R. E. Gresswell (2005), A geostatistical approach for describing spatial pattern in stream networks, *Frontiers Ecol.*, *3*(3), 138–144.

Gardner, K., and R. M. Vogel (2005), Predicting ground water nitrate concentrations from land use, *Ground Water*, *43*(3), 343–352, doi:10.1111/j.1745-6584.2005.0031.x.

Gardner, B., P. J. Sullivan, and A. J. Lembo (2003), Predicting stream temperatures: Geostatistical model comparison using alternative distance metrics, *Can. J. Fish. Aquat. Sci.*, *60*, 344–351, doi:10.1139/f03-025.

Groffman, P. M., G. C. Hanson, E. Kiviat, and G. Stevens (1996), Variation in microbial biomass and activity in four different wetland types, *Soil Sci. Soc. Am. J.*, *60*(2), 622–629.

Groffman, P. M., N. L. Law, K. T. Belt, L. E. Band, and G. T. Fisher (2004), Nitrogen fluxes and retention in urban watershed ecosystems, *Ecosystems*, *7*, 393–403.

Hadas, A., M. Sofer, J. A. E. Molina, P. Barak, and C. E. Clapp (1992), Assimilation of nitrogen by soil microbial population: NH_4 versus organic N, *Soil Biol. Biochem.*, *24*, 137–143, doi:10.1016/0038-0717(92)90269-4.

Hastie, T., R. Tibshirani, and J. Friedman (2001), *The Elements of Statistical Learning*, Springer, New York.

Hill, A. R. (1996), Nitrate removal in stream riparian zones, *J. Environ. Qual.*, *25*, 743–755.

Holloway, J. M., R. A. Dahlgren, B. Hansen, and W. H. Casey (1999), Contribution of bedrock nitrogen to high nitrate concentrations in stream-water, *Nature*, *395*, 785–788.

Holloway, J. M., R. A. Dahlgren, and W. H. Casey (2001), Nitrogen release from rock and soil under simulated field conditions, *Chem. Geol.*, *174*, 403–413, doi:10.1016/S0009-2541(00)00290-4.

Hood, E. W., M. W. Williams, and N. Caine (2003), Landscape controls on organic and inorganic nitrogen leaching across an alpine/subalpine ecotone, Green Lakes Valley, Colorado Front Range, *Ecosystems*, *6*, 31–45, doi:10.1007/s10021-002-0175-8.

Howarth, R. W., D. P. Swaney, E. W. Boyer, R. Marino, N. Jaworski, and C. Goodale (2006), The influence of climate on average nitrogen export from large watersheds in the northeastern United States, *Biogeochemistry*, *79*(1–2), 163–186, doi:10.1007/s10533-006-9010-1.

Jencso, K. G., B. L. McGlynn, M. N. Gooseff, S. M. Wondzell, K. E. Bencala, and L. A. Marshall (2009), Hydrologic connectivity between landscapes and streams: Transferring reach- and plot-scale understanding to the catchment scale, *Water Resour. Res.*, *45*, W04428, doi:10.1029/2008WR007225.

Johnes, P. J., and D. Butterfield (2002), Landscape, regional and global estimates of nitrogen flux from land to sea: Errors and uncertainties, *Biogeochemistry*, *57*, 429–476, doi:10.1023/A:1015721416839.

Kaushal, S. S., and W. M. Lewis (2003), Patterns in the chemical fractionation of organic nitrogen in Rocky Mountain streams, *Ecosystems*, *6*, 483–492, doi:10.1007/s10021-003-0175-3.

Kaushal, S. S., W. M. Lewis, and J. H. McCutchan (2006), Land use change and nitrogen enrichment of a Rocky Mountain watershed, *Ecol. Appl.*, *16*(1), 299–312, doi:10.1890/05-0134.

Kellog, K. S., and V. S. Williams (2005), Geologic map of the Ennis 30′ × 60′ Quadrangle, Madison and Gallatin Counties, Montana, and Park County, Wyoming, *Open File 529*, Mont. Bur. of Mines and Geol., Butte, Mont.

Kendall, C., and J. J. McDonnell (1998), *Isotope Tracers in Catchment Hydrology*, Elsevier, New York.

Legendre, P. (1993), Spatial autocorrelation: Trouble or new paradigm, *Ecology*, *74*, 1659–1673, doi:10.2307/1939924.

Legleiter, C. J., R. L. Lawrence, M. A. Fonstad, W. A. Marcus, and R. Aspinall (2003), Fluvial response a decade after wildfire in the northern Yellowstone ecosystem: A spatially explicit analysis, *Geomorphology*, *54*, 119–136, doi:10.1016/S0169-555X(02)00332-X.

Lipson, D. A., T. K. Raab, S. K. Schmidt, and R. K. Monson (1999), Variation in competitive abilities of plants and microbes for specific amino acids, *Biol. Fertil. Soils*, *29*, 257–261, doi:10.1007/s003740050550.

Lowrance, R., R. Todd, J. Fail Jr., O. Hendrickson Jr., R. Leonard, and L. Asmussen (1984), Riparian forests as nutrient filters in agricultural watersheds, *BioScience*, *34*, 374–377, doi:10.2307/1309729.

McGlynn, B. L. (2005), The role of riparian zones in steep mountain watersheds, in *Global Change and Mountain Regions: An Overview of Current Knowledge*, *Adv. Global Change Res. Ser.*, vol. 23, edited by U. M. Huber, H. K. M. Bugmann, and M. A. Reasoner, pp. 331–342, Springer, New York.

McGlynn, B. L., and J. Seibert (2003), Distributed assessment of contributing area and riparian buffering along stream networks, *Water Resour. Res.*, *39*(4), 1082, doi:10.1029/2002WR001521.

McGuire, K. J., J. J. McDonnell, M. Weiler, C. Kendall, B. L. McGlynn, J. M. Welker, and J. Seibert (2005), The role of topography on catchment-scale water residence time, *Water Resour. Res.*, *41*, W05002, doi:10.1029/2004WR003657.

Meixner, T., A. K. Huth, P. D. Brooks, M. H. Conklin, N. B. Grimm, R. C. Bales, P. A. Haas, and J. R. Petti (2007), Influence of shifting flow paths on nitrogen concentrations during monsoon floods, San Pedro River, Arizona, *J. Geophys. Res.*, *112*, G03S03, doi:10.1029/2006JG000266.

Meyer, J. L., W. H. McDowell, T. L. Bott, J. W. Elwood, C. Ishizaki, J. M. Melack, B. L. Peckarsky, B. J. Peterson, and P. A. Rublee (1988), Elemental dynamics in streams, *J. N. Am. Benthol. Soc.*, *7*, 410–432, doi:10.2307/1467299.

Molenberghs, G., and G. Verbeke (2000), *Models for Discrete Longitudinal Data*, Springer, Berlin.

Montagne, C., L. C. Munn, G. A. Nielsen, J. W. Rogers, and H. E. Hunter (1982), Soils of Montana, *Mont. Agric. Exp. Stn. Bull., 744*, U.S. Dep. of Agric., Bozeman, Mont.

Mueller, D. K., and N. E. Spahr (2006), Nutrients in streams and rivers across the nation—1992–2001, *U.S. Geol. Surv. Sci. Invest. Rep.*, *2006-5107*.

Mulholland, P. J., et al. (2008), Stream denitrification across biomes and its response to anthropogenic nitrate loading, *Nature*, *452*(13), doi:10.1038/nature06686.

National Science Foundation (NSF) (1976), Impacts of large recreational development upon semi-primitive environments, final report, Arlington, Va.

Newson, M. D. (1997), *Land, Water and Development: Sustainable Management of River Basin Systems*, Routledge, London.

Nolan, B. (2001), Relating nitrogen sources and aquifer susceptibility to nitrate in shallow ground waters of the United States, *Ground Water*, *39*(2), 290–299, doi:10.1111/j.1745-6584.2001.tb02311.x.

Peterson, B. J., et al. (2001), Control of nitrogen export from watersheds by headwater streams, *Science*, *292*, 86–90, doi:10.1126/science.1056874.

Peterson, E. E., A. A. Merton, D. M. Theobald, and N. S. Urquhart (2006), Patterns of spatial autocorrelation in stream water chemistry, *Environ. Monit. Assess.*, *121*(1–3), 571–596.

Peterson, E. E., D. M. Theobald, and J. M. Ver Hoef (2007), Geostatistical modeling on stream networks: Developing valid covariance matrices based on hydrologic distance and stream flow, *Freshwater Biol.*, *52*, 267–279, doi:10.1111/j.1365-2427.2006.01686.x.

Post, Buckley, Schuh, and Jernigan, Inc. (2005), 2005 biological monitoring chlorophyll A: Data summary Upper Gallatin water quality restoration planning areas, report, Mont. Dep. of Environ. Quality, Helena, Mont.

Puckett, L. (1994), Nonpoint and point sources of nitrogen in major watersheds of the United States, *U.S. Geol. Surv. Water Resour. Invest. Rep.*, *94-4001*.

Seastedt, T. R., W. D. Bowman, N. Caine, D. McKnight, A. Townsend, and M. W. Williams (2004), The landscape continuum: A model for high-elevation ecosystems, *BioScience*, *54*(2), 111–120, doi:10.1641/0006-3568(2004)054[0111:TLCAMF]2.0.CO;2.

Seibert, J., and B. L. McGlynn (2007), A new triangular multiple flow-direction algorithm for computing upslope areas from gridded digital elevation models, *Water Resour. Res.*, *43*, W04501, doi:10.1029/2006WR005128.

Seitzinger, S. P., R. V. Styles, E. W. Boyer, R. B. Alexander, G. Billen, R. W. Howarth, B. Mayer, and N. Van Breemen (2002), Nitrogen retention in rivers: Model development and application to watersheds in the northeastern U.S.A., *Biogeochemistry*, *57*, 199–237, doi:10.1023/A:1015745629794.

Sickman, J. O., A. L. Leydecker, C. C. Y. Chang, C. Kendall, J. M. Melack, D. M. Lucero, and J. Schimel (2003), Mechanisms underlying export of N from high-elevation catchments during seasonal transitions, *Biogeochemistry*, *64*, 1–24, doi:10.1023/A:1024928317057.

Sigman, D. M., K. L. Casciotti, M. Andreani, C. Barford, M. Galanter, and J. K. Bohlke (2001), A bacterial method for the nitrogen isotopic analysis of nitrate in seawater and freshwater, *Anal. Chem.*, *73*(17), 4145–4153, doi:10.1021/ac010088e.

Simon, K. S., C. R. Townsend, B. J. F. Biggs, and W. B. Bowden (2005), Temporal variation of N and P uptake in 2 New Zealand streams, *J. N. Am. Benthol. Soc.*, *24*(1), 1–18, doi:10.1899/0887-3593(2005)024<0001:TVONAP>2.0.CO;2.

Soil Conservation Service (1978), General soil map, *Ext. Misc. Publ. 16*, U.S. Department of Agriculture, Washington, D. C.

Steffen, W., et al. (2004), *Global Change and the Earth System: A Planet Under Pressure*, Springer, Berlin.

Strahler, A. N. (1952), Hypsometric (area altitude) analysis of erosional topology, *Geol. Soc. Am. Bull.*, *63*, 1117–1142, doi:10.1130/0016-7606(1952)63[1117:HAAOET]2.0.CO;2.

Stumm, W., and J. J. Morgan (1996), *Aquatic Chemistry, Chemical Equilibria and Rates in Natural Waters*, 3rd ed., John Wiley, Hoboken, N. J.

Theobald, D. M., J. B. Norman, E. E. Peterson, and S. B. Ferraz (2005), *FLoWS v1: Functional Linkage of Watersheds and Streams Tools for ArcGIS v9*, Nat. Resour. Ecol. Lab., Colo. State Univ., Ft. Collins, Colo.

Triska, F. J., A. P. Jackman, J. H. Duff, and R. J. Avanzino (1994), Ammonium sorption to channel and riparian sediments: A transient storage pool for dissolved inorganic nitrogen, *Biogeochemistry*, *26*, 67–83, doi:10.1007/BF02182880.

Ver Hoef, J. M., E. E. Peterson, and D. M. Theobald (2006), Spatial statistical models that use flow and stream distance, *Environ. Ecol. Stat.*, *13*, 449–464, doi:10.1007/s10651-006-0022-8.

Vitousek, P. M., J. R. Gosz, C. C. Grier, J. M. Melillo, W. A. Reiners, and R. L. Todd (1979), Nitrate losses from disturbed ecosystems, *Science*, *204*, 469–474, doi:10.1126/science.204.4392.469.

Vogel, R. M., I. Wilson, and C. Daly (1999), Regional regression models of annual streamflow of the United States, *J. Irrig. Drain. Eng.*, *125*, 148–157, doi:10.1061/(ASCE)0733-9437(1999)125:3(148).

Wetzel, R. G. (2001), *Limnology*, 3rd ed., Academic, San Diego, Calif.

Whitehead, P. G., P. J. Johnes, and D. Butterfield (2002), Steady state and dynamic modelling of nitrogen in River Kennet: Impacts of land use change since 1930s, *Sci. Total Environ.*, *282–283*, 417–434, doi:10.1016/S0048-9697(01)00927-5.

Williams, M. W., and J. M. Melack (1991), Solute chemistry of snowmelt and runoff in an alpine basin, Sierra Nevada, *Water Resour. Res.*, *27*, 1576–1588.

Williams, M. W., and K. A. Tonnessen (2000), Critical loads for inorganic nitrogen deposition in the Colorado Front Range, USA, *Ecol. Appl.*, *10*, 1648–1665, doi:10.1890/1051-0761(2000)010[1648:CLFIND]2.0.CO;2.

Williams, M. W., A. D. Brown, and J. M. Melack (1993), Geochemical and hydrologic controls in the composition of surface water in a high-elevation catchment, Sierra Nevada, California, *Limnol. Oceanogr.*, *38*(4), 775–797.

Yuan, L. L. (2004), Using spatial interpolation to estimate stressor levels in unsampled streams, *Environ. Monit. Assess.*, *94*, 23–38, doi:10.1023/B:EMAS.0000016877.52279.05.

Zimmermann, B., H. Elsenbeer, and J. M. De Moraes (2006), The influence of land-use changes on soil hydraulic properties: Implications for runoff generation, *For. Ecol. Manage.*, *222*(1–3), 29–38, doi:10.1016/j.foreco.2005.10.070.

K. K. Gardner and B. L. McGlynn, Department of Land Resources and Environmental Sciences, Montana State University, Bozeman, MT 59716, USA. (kristin.k.gardner@gmail.com)